Graphene Coupled with Nanocrystals: Opportunities and Challenges for Energy and Sensing Applications

ARTICLE *in* JOURNAL OF PHYSICAL CHEMISTRY LETTERS · JULY 2013

Impact Factor: 7.46 · DOI: 10.1021/jz400976a

4 AUTHORS, INCLUDING:

Shumao Cui
University of Wisconsin - Milwaukee
64 PUBLICATIONS **1,508** CITATIONS
SEE PROFILE

Shun Mao
University of Wisconsin - Milwaukee
85 PUBLICATIONS **2,382** CITATIONS
SEE PROFILE

Ganhua Lu
University of Wisconsin - Milwaukee
65 PUBLICATIONS **2,640** CITATIONS
SEE PROFILE

THE JOURNAL OF PHYSICAL CHEMISTRY Letters

Perspective

pubs.acs.org/JPCL

Graphene Coupled with Nanocrystals: Opportunities and Challenges for Energy and Sensing Applications

Shumao Cui,[†,§] Shun Mao,[†,§] Ganhua Lu,[‡,§] and Junhong Chen*[,†]

[†]Department of Mechanical Engineering, University of Wisconsin—Milwaukee, 3200 North Cramer Street, Milwaukee, Wisconsin 53211, United States

[‡]Department of Mechanical Engineering, University of Alaska Anchorage, 3100 Providence Drive, Anchorage, Alaska 99508, United States

ABSTRACT: Graphene coupled with nanocrystals (NCs) represents a new type of hybrid nanostructure that has attracted wide attention in energy and sensing applications. The interaction between graphene and NCs provides the hybrids with additional properties, offering rich opportunities to tune the material structure and properties. This Perspective highlights some recent progress in the research on graphene–NC hybrid structures with a focus on their energy storage/conversion and sensing applications. The structural characteristics of graphene–NC hybrids and the advantages of coupling NCs with graphene are demonstrated and discussed. Recent studies have shown the great potential of graphene–NC hybrids to improve the performance of energy storage/conversion devices (e.g., Li ion batteries, supercapacitors, fuel cells, and solar cells) and sensing devices (e.g., chemical sensors, biosensors, and water sensors). Further understanding and development of graphene–NC hybrids could therefore help address the demand for new energy storage/conversion systems and challenges for the widespread use of graphene-based sensors.

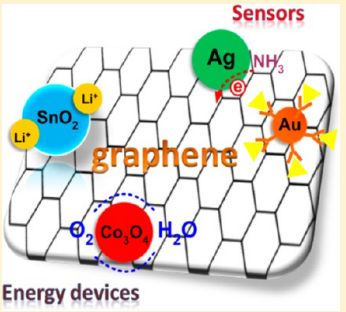

The past decade has witnessed an explosive growth of research interest in graphene,[1,2] a one-atom-thick layer of sp^2-bonded carbon atoms arranged in a two-dimensional (2D) honeycomb lattice structure. While graphene itself has exceptional electrical,[1,2] thermal,[3] and mechanical[4] properties and holds huge potential for various applications (e.g., field effect transistors (FETs), sensors, electrochemical capacitors/supercapacitors, lithium ion batteries (LIBs), fuel cells, and solar cells),[5] graphene is also a "wonder-land" perfect for combining with other functional nanomaterials to form hybrid nanostructures with properties tailored for intended applications. Graphene-based hybrid materials open up new frontiers in science and technology and expand the scope of graphene's applications as synergetic effects can result from the interaction between graphene and the nanomaterials supported on graphene. Graphene decorated with nanocrystals (NCs) is such a graphene-based hybrid material.[6] NCs with sizes between 1 and 100 nm have unique electronic, optical, magnetic, mechanical, and chemical properties that differ from those of both their constituent atoms/molecules and their corresponding bulk materials. Graphene–NC hybrid structures could potentially display not only the unique properties of NCs[7,8] and those of graphene[9−11] but also additional novel physical and chemical properties due to the interaction between graphene and attached NCs.

An increasing demand for energy and a pressing need for alternatives to conventional fossil fuels have stimulated considerable efforts to develop novel materials to address challenging problems in clean/renewable energy production, conversion, and storage. Graphene–inorganic nanocomposites (e.g., graphene–NC hybrids) have been considered as one of the promising alternatives as electrode materials in energy devices due to the superior electrical conductivity, high specific surface area, and good chemical stability of graphene and high electrochemical/electrocatalytic activities from NCs. Recent studies have shown that electrode materials based on graphene–NC hybrids could considerably improve the performance (i.e., higher power/energy densities, higher efficiency, and better cycling/rate performance) of energy storage/conversion devices (e.g., supercapacitors, LIBs, fuel cells, and solar cells).[12−14] On the other hand, graphene-based nanostructures have been widely studied for sensing applications (e.g., gas sensors,[15,16] biosensors,[17] and water sensors[18]) due to their high electron mobility, large specific surface area, and high sensitivity to electronic perturbations from gas/bio/chemical-molecule adsorption on their surfaces.

Graphene-based hybrid materials open up new frontiers in science and technology and expand the scope of graphene's applications as synergetic effects can result from the interaction between graphene and the nanomaterials supported on graphene.

Received: May 10, 2013
Accepted: July 11, 2013

   dx.doi.org/10.1021/jz400976a | *J. Phys. Chem. Lett.* 2013, 4, 2441−2454

NCs in a graphene–NC sensor could work as a sensitivity promoter, a selectivity tuner, or a molecule linker; in all aspects, hybrid graphene–NC sensors show improved sensing performance compared with those using bare graphene.[15,16]

We note that many reviews have summarized the up-to-date achievements of graphene-based composites and their applications in energy and sensing devices. For example, in one review,[19] Lightcap et al. reviewed the recent advances of graphene-based composites in solar energy devices, that is, solar cells, and as the surface-enhanced Raman scattering (SERS) substrates for trace molecule detection. In another review,[20] Huang et al. discussed the graphene–inorganic and –organic composites, their synthetic methods, and applications in energy devices. However, no review has focused on graphene–NC hybrids and their applications in both energy and sensing devices (electronic sensors). In this Perspective, we highlight some recent progress in the research on graphene–NC hybrid structures with an emphasis on the use of these hybrid nanomaterials for energy storage/conversion devices and sensors. Some important aspects of graphene–NC hybrid structures are discussed, including the structural characteristics, the interactions between NCs and graphene, advantages of hybrid structures, and their excellent performance as electrode materials/catalysts in energy devices and sensing elements in sensors. Combining graphene with NCs provides a viable option to develop novel hybrid nanomaterials for energy devices and sensors.

Combining graphene with NCs provides a viable option to develop novel hybrid nanomaterials for energy devices and sensors.

Graphene–NC Hybrids for Energy Storage/Conversion Applications. Graphene–NC Hybrids for Energy Storage Devices. An electrochemical capacitor (EC) or a supercapacitor is a type of energy storage device that has high power density and long cycle life.[21] Depending on the charge storage mechanism as well as the active materials used, ECs can be categorized into three types, electric double-layer capacitors (EDLCs), pseudocapacitors, and hybrid ECs. EDLCs store charges electrostatically via reversible ion adsorption at the electrode/electrolyte interface; therefore, graphene is expected to have excellent EDLC properties due to its high theoretical surface area (2630 $m^2 \cdot g^{-1}$)[22] and high conductivity.[11] Supercapacitors based on reduced graphene oxide (RGO) were demonstrated to have a capacitance of ~130 and ~100 $F \cdot g^{-1}$ in aqueous KOH and organic electrolytes, respectively.[22] Recently, the specific capacitance of graphene was reported to reach 484 $F \cdot g^{-1}$ (at a current density of 0–100 $A \cdot g^{-1}$) in an aqueous electrolyte;[23] however, this value is still below the intrinsic capacitance of a single-layer graphene sheet (~21 $\mu F \cdot cm^{-2}$,[24] or ~550 $F \cdot g^{-1}$). The limited capacitance is mainly due to the agglomeration/restacking of graphene sheets, which greatly reduces the accessible surface area of graphene.

On the other hand, metal oxide or hydroxide NCs are typically used as active pseudocapacitive materials because of their high theoretical specific capacitance. However, the conductivity of these materials is relatively low, limiting the energy storage capacity. An effective way to increase the capacity is to deposit these pseudocapacitive materials on a support that is highly conductive, has a high specific surface area, and is electrochemically stable. Graphene has the desirable properties to be an ideal support for pseudocapacitive materials. Therefore, by combining graphene and pseudocapacitive NCs, it is anticipated that a high-performance capacitor can be obtained as a result of both EDLC and pseudocapacitor mechanisms. In those hybrid materials, graphene sheets are prevented from aggregation/restacking due to the hybrid structure and work as the conductive support.

So far, various metal oxide or hydroxide NCs have been used in graphene-based supercapacitors, including MnO_x, Co_3O_4, SnO_2, Fe_3O_4, $Ni(OH)_2$, and $Co(OH)_2$,[25] and the incorporation of those NCs could enhance the specific capacitance beyond that of bare graphene as well as the stability during reversible charging/discharging processes. Among those NCs, MnO_x is one of the most promising electrode materials for supercapacitor applications due to its high theoretical specific capacitance ($C_{sp} \approx 1370$ $F \cdot g^{-1}$) and low cost.[26]

Recently, we reported on a crumpled graphene (CG)–Mn_3O_4 hybrid that was produced by direct aerosolization of a graphene oxide (GO) suspension mixed with precursor ions.[13] As a proof of concept (Figure 1), we demonstrated the use of CG–Mn_3O_4 in an electrochemical supercapacitor, and the specific capacitance could reach as high as 1027 $F \cdot g^{-1}$ at a current density of 5 $A \cdot g^{-1}$.[13] In this study, GO sheets were shrunk and compressed into a crumpled ball shape with rapidly evaporating solvents in a tube furnace, and NCs spontaneously grew from precursor ions and assembled on both external and internal surfaces of CG balls. The crumpled ball structure makes it possible to fully use the surface area of the graphene sheet and avoids the agglomeration/restacking of graphene sheets on the current collector.

In another report,[27] solution-exfoliated graphene sheets were first coated on three-dimensional, porous textiles supports (microfibers); a hybrid graphene/MnO_2-based textile was then created with the subsequent electrodeposition of pseudocapacitive MnO_2 NCs. As shown in Figure 2, the three-dimensional (3D) network not only permitted high loading of active materials but also facilitated the access of electrolyte to the electrodes. In this work, the gaphene–MnO_2 composites yielded a specific capacitance up to 315 $F \cdot g^{-1}$ and excellent cycling performance of ~95% capacitance retention over 5000 cycles.

Very recently, He et al. reported a 3D and flexible graphene network on Ni foam with MnO_2 loading.[28] The hybrid graphene–MnO_2 structure is similar to that in the previous report, but the rigid microfiber support was replaced with flexible Ni foam. With the flexible and porous structure, the loading of active MnO_2 on the graphene could be very high (9.8 $mg \cdot cm^{-2}$, ~92.9% of the mass of the entire electrode), and the device showed a high area capacitance of 1.42 $F \cdot cm^{-2}$ at a scan rate of 2 $mV \cdot s^{-1}$ and a specific capacitance of 130 $F \cdot g^{-1}$ with optimized MnO_2 content. In general, the accessible surface area could be increased with the deposition of NCs on graphene because of the unique hybrid structure, and the ion transport could be enhanced, leading to improved capacitor performance. In addition, good cycling performance in the capacitance could be achieved using the hybrid structure because the agglomeration and loss of NCs during the charge/discharge could be effectively inhibited.

LIBs are attractive for energy storage due to their high energy densities that enable them to be the dominant power source of

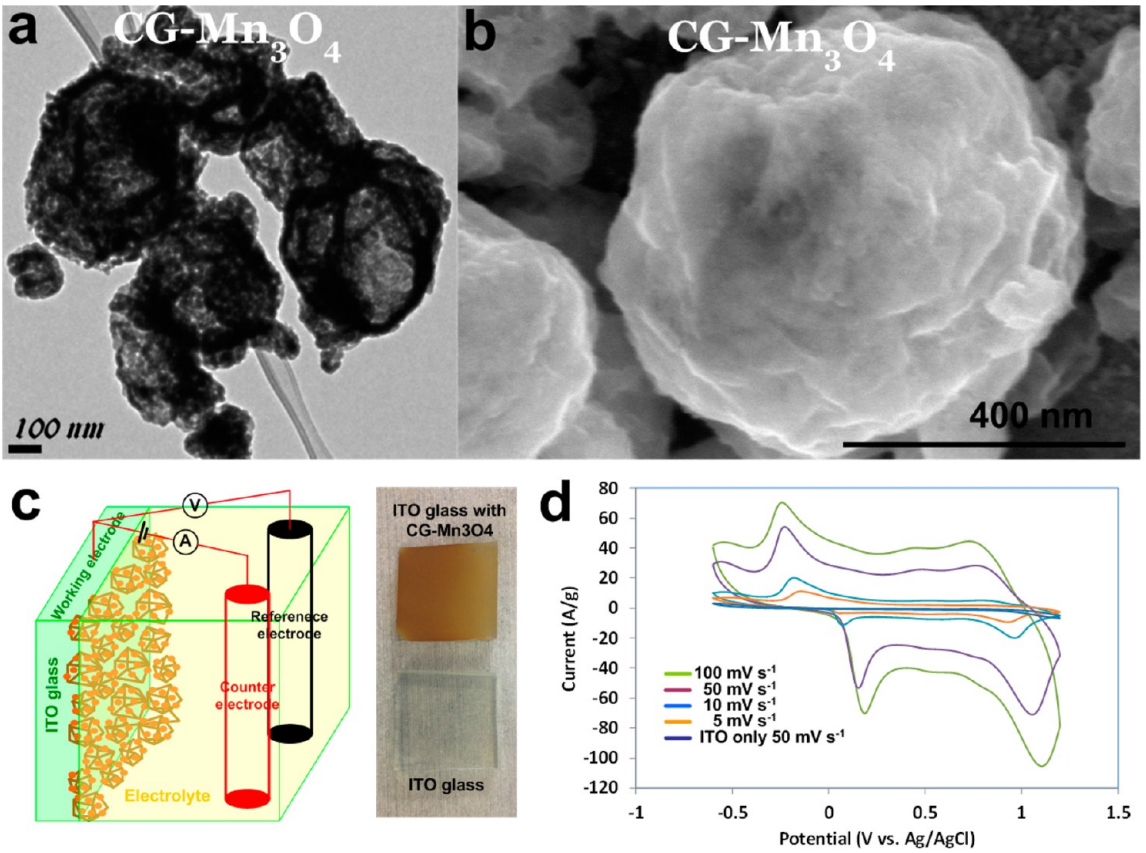

Figure 1. (a) Transmission electron microscopy (TEM) and (b) scanning electron microscopy (SEM) images of CG−Mn_3O_4 hybrid structures. (c) Schematic of the capacitor test for CG−Mn_3O_4 NC hybrid electrodes in a 1 M Na_2SO_4 aqueous electrolyte; the digital picture shows the ITO glass before and after coating CG−Mn_3O_4 NC hybrids. (d) Cyclic voltammetry (CV) for CG−Mn_3O_4 at different scan rates (the CV curve for ITO-only at a scan rate of 50 mV·s^{-1} is included for comparison). Reprinted from ref 13.

high-end consumer electronic products (e.g., laptops, cell phones, and cameras) and hold tremendous potential for powering next-generation electric vehicles (EVs).[29] The energy density and performance of LIBs largely depend on the physical and chemical properties of cathode and anode materials. To further improve the battery performance and to meet the growing energy storage requirements, various alternative materials have been explored, and new anode materials superior to the commercial anode material graphite (theoretical capacity: 372 mA·h·g^{-1}) have drawn great attention in recent years.

Graphene has been theoretically proved to have a higher lithium storage capacity (744 mA·h·g^{-1})[30] than graphite. However, similar to supercapacitor applications, graphene sheets tend to restack and therefore lose their high specific surface area and intrinsic chemical and physical properties. Inorganic materials, such as Sn, SnO_2, FeO_x, and Si, have been demonstrated as potential anode materials for LIBs due to their higher specific capacities than graphite (981 mA·h·g^{-1} for Sn, 1491 mA·h·g^{-1} for SnO_2, ∼1000 mA·h·g^{-1} for FeO_x, and 4200 mA·h·g^{-1} for Si).[31−33] Therefore, incorporating inorganic NCs with a high lithium storage capacity on graphene sheets has been proposed, and the prepared hybrids have shown a higher lithium storage capacity than bare graphene or commercial graphite.[14,34]

Silicon has been widely investigated as a high-performance anode material for LIBs due to its abundance in nature, its low working potential, and its highest known theoretical specific capacity of ∼4200 mA·h·g^{-1} (more than 10 times higher than that of graphite). However, Si suffers from a dramatic volume change (∼400%) during the lithium insertion and extraction, leading to severe pulverization and electrical disconnection from the current collector and, thus, performance degradation.[35] To address this challenge, a graphene−Si hybrid structure has been proposed. Zhao et al. reported a sandwich structure constructed with graphene sheets and Si NCs in between (Figure 3).[34] This structure enabled the easy ion transport through the graphene layers with new diffusion channels created within the graphene layers, overcoming the high resistance of graphene materials for Li ion transport due to their extreme width-to-thickness aspect ratio and intersheet aggregation. In addition, the high flexibility of graphene sheets and voids between neighboring sheets could effectively accommodate the volume change of embedded Si NCs during charge/discharge processes. This graphene−Si composite electrode achieved an unprecedented reversible capacity of 3200 mA·h·g^{-1} at 1 A·g^{-1} and excellent stability for over 150 cycles.

In addition to Si, Sn-based materials (e.g., Sn and SnO_2) are another type of appealing and competitive candidate as the anode material of LIBs, in which lithium can be reversibly alloyed/dealloyed with Sn for a high specific capacity at low potential. We have developed a simple method to synthesize Sn-based NC−graphene hybrids through simultaneous growth of SnO_2 NCs and a carbonaceous polymer film on GO sheets followed by heat treatment.[14] The porosity in the sandwich-structured Sn−C hybrids offered space to accommodate a large volume change of NCs while maintaining the electrode

dx.doi.org/10.1021/jz400976a | J. Phys. Chem. Lett. 2013, 4, 2441−2454

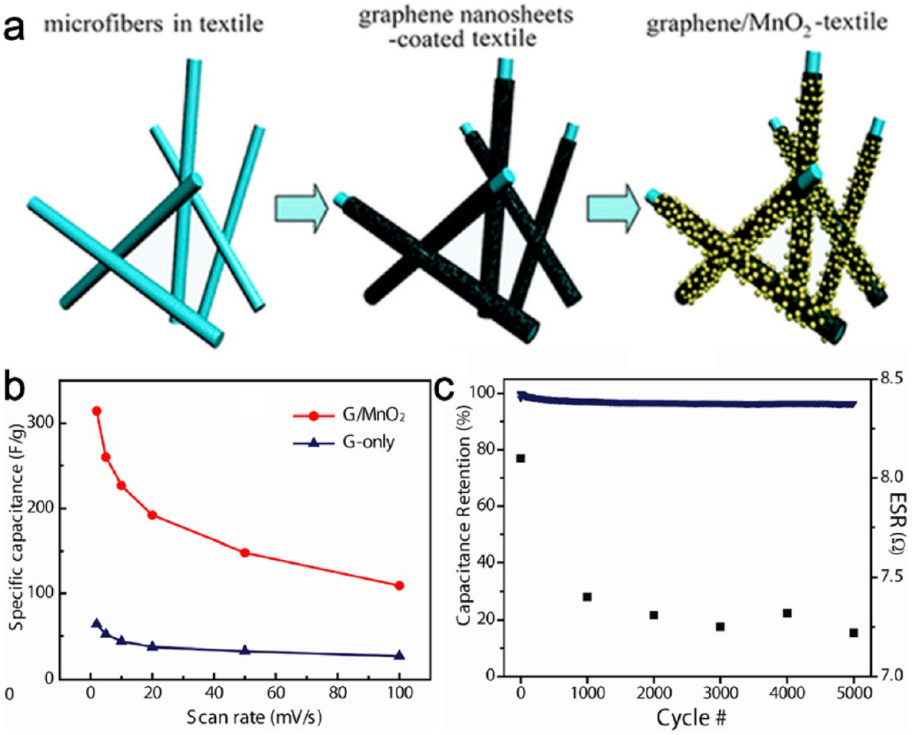

Figure 2. (a) Schematic of two key steps for preparing hybrid graphene/MnO_2-nanostructured textiles as high-performance EC electrodes. (b) Comparison of specific capacitance values between graphene/MnO_2 textile and graphene nanosheets-only textile at different scan rates. (c) Cycling performance of hybrid ECs showing capacitance retention of ∼95% after 5000 cycles of charging and discharging at a current density of 2.2 A/g and subtle change in EC's equivalent series resistance taken from impedance measurements every 1000 cycles. Reprinted from ref 27.

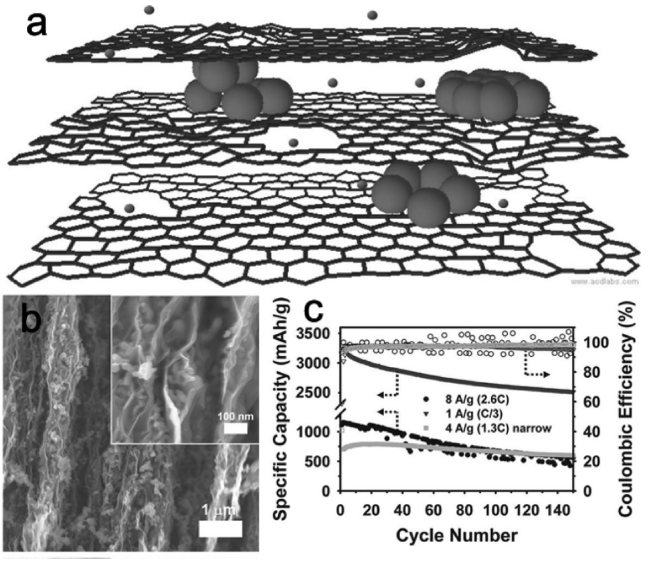

Figure 3. (a) Schematic of a composite electrode material constructed with a graphene scaffold with in-plane carbon vacancy defects. Electrochemically active components (Si NCs (large spheres)) are sandwiched between graphene sheets to interconnect graphitic domains. (b) SEM image of the cross section of the graphene−Si composite; the inset shows Si NCs embedded between graphene sheets uniformly. (c) Specific delithiation capacity (solid) and Coulombic efficiency (open) of Ar-reduced Si−graphene between 0.02 and 1.5 V at 1 and 8 $A{\cdot}g^{-1}$ (C/3 and 2.6 C based on a theoretical capacity of 3052 $mAh{\cdot}g^{-1}$) and between 0.1 and 0.55 V at 4 $A{\cdot}g^{-1}$ (1.3 C). Reprinted with permission from ref 34. Copyright Wiley-VCH, 2011.

integrity during cycling. The best anode reported in this study achieved a high initial capacity of 1616.2 $mA{\cdot}h{\cdot}g^{-1}$ and a 43.2% loss in the second cycle and maintained a capacity of 565.1 $mA{\cdot}h{\cdot}g^{-1}$ after 50 charge/discharge cycles.

To enhance the battery performance in terms of the specific capacity and stability during the cycling tests, the graphene−NC sandwich structure has proved to be promising because this structure could prevent the restacking of graphene sheets as well as the agglomeration and loss of NCs. On the other hand, a 3D porous graphene structure has also been studied and could lead to significantly enhanced battery performance. Chio et al. reported a high-performance LIB anode material based on a 3D heterostructured architecture consisting of Co_3O_4 NCs deposited on porous graphene.[36] They used polystyrene spheres as sacrificial templates to produce porous structures of graphene with tunable pore sizes ranging from 100 nm to 2 μm. This unique heterogeneous 3D structure provided excellent Li^+ ion storage/release capability and displayed good battery performance with a high rate capability of 71% retention (initial capacity: 1285 $mA{\cdot}h{\cdot}g^{-1}$) at a current rate of 1 $A{\cdot}g^{-1}$ and a good cycling performance with 90.6% retention after 50 cycles. A wide range of NCs (e.g., Si-based NCs,[37] Sn-based NCs,[14] FeO_x,[38] and CoO_x)[39] have been combined with graphene as high-performance anode materials for the next-generation LIBs.

Graphene−NC Hybrids for Energy Conversion Devices. An electrolyte membrane fuel cell,[40] a device relying on electrochemical oxidation of hydrogen and reduction of oxygen, is one promising technology for sustainable and green energy supply. Electrocatalysts for the oxygen reduction reaction (ORR) are a key factor for this clean energy technology, and intense research has been conducted to explore low-cost and high-efficiency

dx.doi.org/10.1021/jz400976a | J. Phys. Chem. Lett. 2013, 4, 2441−2454

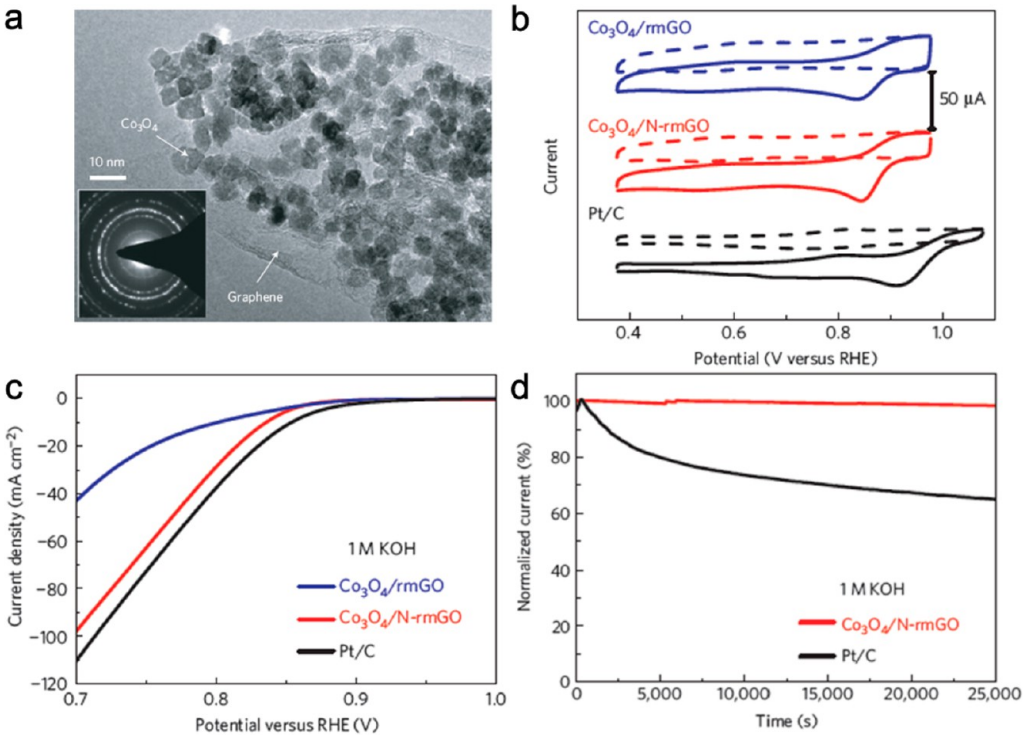

Figure 4. (a) TEM image of Co_3O_4–N-rmGO hybrids (inset: SAD pattern). (b) CV curves of Co_3O_4–rmGO hybrids, Co_3O_4–N-rmGO hybrids, and Pt/C on glassy carbon electrodes in O_2-saturated (solid line) or Ar-saturated 0.1 M KOH (dash line). (c) Oxygen reduction polarization curves of Co_3O_4–rmGO hybrids, Co_3O_4–N-rmGO hybrids, and Pt/C dispersed on carbon fiber paper in O_2-saturated 1 M KOH. (d) Chronoamperometric responses (percentage of current retained versus operation time) of Co_3O_4–N-rmGO hybrids and Pt/C on carbon fiber paper electrodes kept at 0.70 V versus RHE in O_2-saturated 1 M KOH. Reprinted with permission from ref 12. Copyright Macmillan Publishers Ltd., 2011.

electrocatalysts to replace traditionally used carbon-supported platinum (Pt/C). Due to the high cost of Pt and declining activity over operation, alternative catalysts based on Pt alloys,[41] nonprecious metal/metal composites (e.g., Fe- or Co-based catalysts),[42] and metal-free materials (e.g., conducting polymer,[43] CNTs,[44] and graphene)[45] have been actively investigated. With a high specific surface area and conductivity, graphene has been used as a support for ORR catalysts, replacing carbon black. Meanwhile, catalysts with only graphene or nitrogen-doped graphene have also been reported because edges, folds, and defects in graphene could also work as catalytic sites for ORR.[46]

For graphene–NC-based catalysts, nonprecious metal/metal composites and metal-free materials have been widely studied. Among those hybrid structures, one of the best ORR catalysts in alkaline solutions is Co_3O_4 NCs supported on graphene, reported by Dai's group in 2011 (Figure 4).[12] Co_3O_4 itself is a material with little ORR activity; however, Co_3O_4 NCs grown on reduced mildly oxidized GO (rmGO) exhibited high ORR performance in alkaline solutions. The prepared rmGO–Co_3O_4 hybrid exhibited ORR catalytic activity comparable to that of a commercial Pt/C catalyst (20 wt % Pt on Vulcan XC-72) and superior stability. In this study, N-doped rmGO has also been prepared by adding NH_4OH; the bond formation between Co_3O_4 and N-rmGO (interfacial Co–O–C and Co–N–C bonds) and changes in the chemical bonding environment for C, O, and Co atoms in the hybrid material were found to be responsible for the synergistic ORR catalytic activity.

In other cases, metal-free NCs were also reported for electrocatalytic applications, having the advantages of low cost and environmental friendliness. A typical example of this is RGO–CN nanohybrids,[47] which exhibited excellent electrocatalytic ORR performance, in terms of electrocatalytic activity and long-term durability. Several factors determine the catalyst performance in ORR. First, the support material (graphene/RGO) should be highly conductive to promote the electron transfer from the electrode. Second, the edges and defects in graphene/RGO may work as catalytic sites for ORR; in this case, the graphene/RGO works not only as the conductive support but also as the catalyst itself. From this point of view, a highly reduced GO may be a better choice as the NC support because it is highly conductive and edge/defect-rich. Third, the hybrid structure should be robust enough to sustain its structure during ORR, which could be achieved by in situ growth/deposition of NCs on the graphene surface or by creating a graphene-wrapping structure.

Photovoltaic cells or solar cells have been widely studied as renewable energy-harvesting systems capable of converting solar radiation directly into electricity by the photovoltaic effect. Because of the high electron mobility, the excellent optical transparency of graphene, and the tunable band gap of semiconducting NCs, graphene–NC hybrids present a new opportunity for the fabrication of fascinating electrode materials in solar cells, for example, in dye-sensitized solar cells (DSSCs) and quantum-dot-sensitized solar cells (QDSSCs). Significant progress in recent years has been made toward the synthesis of graphene–semiconducting NC composites with various NCs, for example, TiO_2, CdSe, and CdS.[48,49] In QDSSCs, QDs such as CdSe and CdS with a large extinction coefficient and a tunable band gap (by changing the QD size) could harvest light energy and transfer excited electrons to graphene films. Several groups have obtained graphene–QD hybrid nanostructures by

dx.doi.org/10.1021/jz400976a | J. Phys. Chem. Lett. 2013, 4, 2441–2454

using wet chemical methods, and much effort has been devoted to understanding the photoinduced charge transfer from QDs to graphene.[19]

Our group[50] used a chemical vapor deposition (CVD) method to produce graphene–CdSe NC hybrids, in which CdSe NCs can be selectively attached to graphene sheets without any chemical linkers. Upon visible light excitation, the graphene–CdSe NC hybrids showed significantly faster photoresponse compared with the pure CdSe NC film; moreover, the photoresponse amplitude and time can be modulated by the chemical environment and the NC coverage on graphene (Figure 5). The hybrid structure with low CdSe

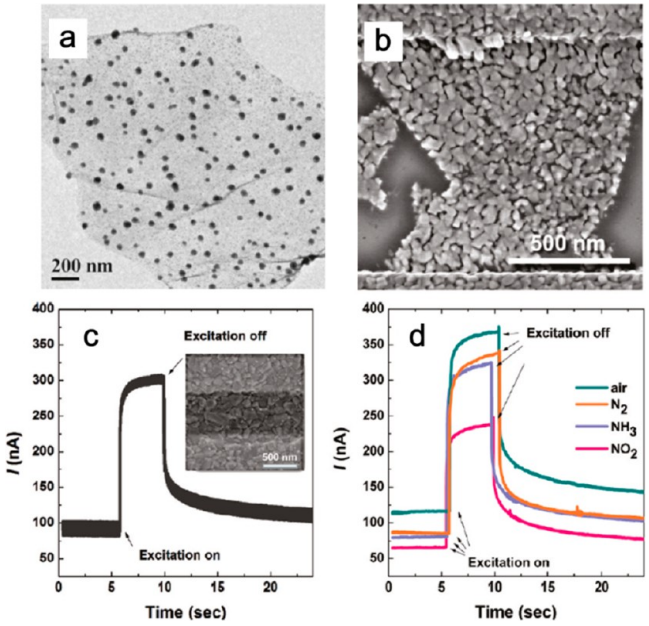

Figure 5. (a) TEM image of graphene–CdSe NC hybrids. (b) SEM image of a high-coverage NC photodetector. Photoinduced current response versus time of a high-coverage NC photodetector under irradiation of (c) simulated sunlight at 100 mW·cm^{-2} in air and (d) a 532 nm laser of ~50 mW with different gas flows of air, N_2, NH_3, and NO_2. The inset of (c) is an SEM image of the corresponding device. All current changes were recorded with a bias voltage of 0.01 V. Reprinted from ref 50.

NC coverage showed distinct photoresponse times in air, N_2, NH_3, and NO_2, while high CdSe NC coverage led to a nearly constant but 3 orders of magnitude smaller response time in all gaseous environments. This study could help to understand the transfer of photogenerated charge carriers between QDs and graphene, thus paving the way for practical applications of graphene and hybrid graphene–QD structures in optoelectronic devices.

On the other hand, graphene–NC hybrids could also be used in DSSCs as cost-effective alternative catalysts to Pt counter electrodes. In another report,[51] our group has demonstrated nitrogen-doped graphene (NG)–TiN nanohybrids as catalysts for the counter electrode of DSSCs. Due to the excellent catalytic properties of TiN NPs and the high electrical conductivity of graphene, the hybrids showed slightly better electrochemical catalytic performance than Pt for I^{3-} reduction. Specifically, the NG–TiN-based DSSC displayed 20% higher short-circuit current density and a slightly higher power conversion efficiency (5.78%) than the Pt counter electrode cell (5.03%). The reported NG–TiN nanohybrids can be used as a low-cost counter electrode to replace Pt in DSSCs. Graphene–NC hybrids have demonstrated great potential in either photoelectrodes or counter electrodes of solar cells and are one of the most promising electrode materials for next-generation high-efficiency and low-cost solar cells.

Graphene–NC Hybrids for Sensing Applications. Graphene–NC Hybrids for Gas Sensors. Intrinsic graphene is sensitive to changes of its chemical environment due to its high specific surface area, high carrier mobility, and low electrical noise at room temperature.[52] However, the sp^2 carbon–carbon bonds in graphene are chemically stable, resulting in a relatively weak interaction between graphene and many gas molecules (e.g., H_2 and CO). Although graphene is responsive to certain gases (e.g., NO_2 and NH_3) diluted in helium or nitrogen at very low concentrations,[53,54] the selectivity is poor, and the recovery time is extremely long,[52] which limits its use in practical sensing applications. Functionalizing graphene with NCs is an effective method to tune the sensitivity, selectivity, and dynamic response of graphene-based gas sensors.

Generally, two types of NCs are used to decorate graphene for sensing enhancement, noble metal NCs and metal oxides NCs. Noble metals (e.g., Au, Ag, Pt, and Pd), which have been widely used as catalysts, are applied to sensitive and selective gas sensors because they can selectively promote reactions involving gas molecules. Inspired by our previous experimental and theoretical results that suggest Ag NC-decorated carbon nanotubes (CNTs) can be used for fast and selective detection of ammonia,[55] we have recently developed high-performance ammonia sensors using Ag NC-decorated RGO (RGO/Ag) hybrids fabricated in a controllable fashion.[56] Ag NCs were first synthesized by physical vaporization of solid Ag precursors using a mini-arc plasma source and then deposited onto RGO using the electrostatic force-directed assembly, during which the NC loading density can be controlled by the deposition time. Figure 6a shows the as-synthesized RGO/Ag hybrid with Ag NCs being uniformly distributed on the RGO sheet, which

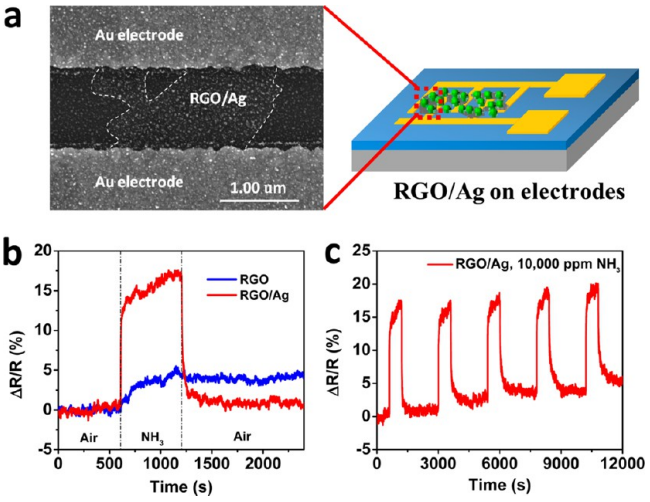

Figure 6. (a) SEM image of a Ag NC-decorated RGO bridging a pair of gold electrode fingers and a schematic of the RGO/Ag hybrid sensor. (b) Room-temperature dynamic-sensing responses of RGO before and after Ag NC deposition. (c) Five-cycle responses of RGO/Ag to 10 000 ppm NH_3, indicating a good stability of the sensor. Reprinted from ref 56 by permission of The Royal Society of Chemistry (RSC).

dx.doi.org/10.1021/jz400976a | J. Phys. Chem. Lett. 2013, 4, 2441–2454

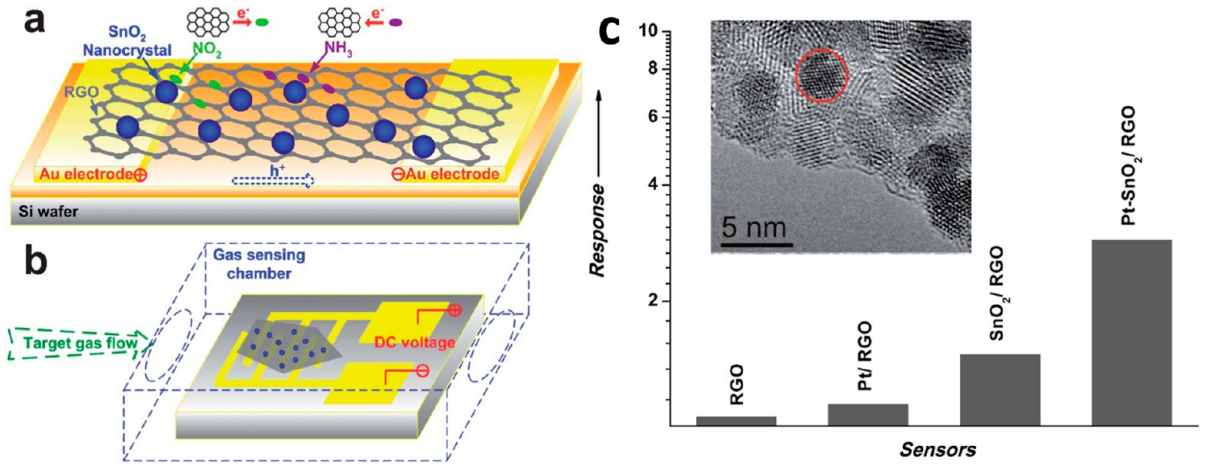

Figure 7. (a) Schematic of the RGO/SnO_2 gas-sensing platform. (b) Schematic of the sensor testing system. Reprinted from ref 15 by permission of The Royal Society of Chemistry (RSC). (c) Comparison of the responses of the Pt−SnO_2/RGO and RGO sensors to 1% H_2 in air; the inset is a high-resolution TEM image of Pt−SnO_2/RGO. Reprinted with permission from ref 57. Copyright Wiley-VCH, 2012.

bridges a pair of gold electrodes. The sensing performance of the RGO (i.e., sensitivity, response, and recovery) is improved significantly by comparing the sensing signals before and after Ag NC decoration (Figure 6b). The hybrid sensor is quite stable, as evidenced by several repeatable sensing cycles (Figure 6c). In the RGO/Ag hybrid structure, Ag NCs serve as the dominant sensing elements due to the fast and selective interaction between Ag NCs and NH_3. Both the adsorption of NH_3 on Ag and the electron transfer between Ag NCs and NH_3 are fast, facilitating a rapid change of charge carrier concentration (holes) in RGO and thus resulting in a fast response. The RGO/Ag hybrids also have higher sensitivity than Ag NC-decorated multiwalled carbon nanotubes (MWCNTs), which could be attributed to the larger specific surface area of RGO for NC deposition than MWCNTs.

Metal oxide (e.g., widely used SnO_2) NCs have also been used to functionalize graphene to improve the gas-sensing performance. Our group reported a novel gas-sensing platform of SnO_2 NC-decorated RGO with tunable sensing performance (Figure 7a and b).[15] When gas molecules adsorb on the hybrids, the electron transfer between RGO/SnO_2 hybrids and gaseous molecules (e.g., NH_3 and NO_2) leads to a conductance change of the hybrids. Comparing the sensing data of bare RGO and RGO/SnO_2 hybrids clearly indicates that the sensing performance of RGO can be modulated by SnO_2 NCs, namely, an enhanced sensing signal toward NO_2 with a weakened signal toward NH_3. The repeatability results show that with SnO_2 deposition, the sensitivity of RGO increased from 2.16 to 2.87 for 100 ppm NO_2, while it decreased from 1.46 to 1.12 for 1% NH_3. The enhancement in selectivity could be attributed to p−n junctions formed at the interface between RGO (p-type) and SnO_2 (n-type) NCs that could effectively modulate the electronic-transfer process.

With the success of RGO/NC binary gas sensors, introducing an appropriate additional NC phase to form a ternary system can be expected to further improve the sensing properties of graphene. Russo et al. have developed hybrids of RGO functionalized with SnO_2 and Pt NCs (Pt−SnO_2/RGO) (inset of Figure 7c) using a simple, fast, and readily scalable microwave-assisted method for H_2 detection.[57] Sensors with the Pt−SnO_2/RGO hybrids showed performance superior to the corresponding pure and binary systems for 1% H_2 detection at a low temperature (50 °C) (Figure 7c). The sensitivity of the RGO is quite low, indicating a weak interaction between the RGO and H_2. It is well-known that pure graphene is insensitive to H_2; the observed response from the RGO could be attributed to the remaining functional groups (e.g., epoxide and carboxylic) on the RGO surface. Among those tested materials, Pt−SnO_2/RGO hybrids had the best sensing performance with the highest sensitivity to different concentrations of H_2 from 0.5 to 3.0%, with the shortest response and recovery times of 3−7 and 2−6 s, respectively. The outstanding performance of the Pt−SnO_2/RGO hybrids is attributed to the heterojunction formed between the n-type SnO_2 and the p-type RGO and the catalytic effect of Pt NCs for dissociating H_2. The selectivity study of Pt−SnO_2/RGO shows that the hybrids were insensitive to the other reducing gases (CO and methane), and the presence of Pt NCs in the hybrids reduced the response to NO_2 while increasing the response to H_2, resulting in a highly selective hydrogen sensor.

To achieve high sensitivity and selectivity for a graphene−SnO_2 gas sensor, doping SnO_2 NCs is another effective method. The charge carrier concentration of the semiconducting SnO_2 can be dramatically increased by dopants, which facilitates the electron transfer during the interaction with gases. Dopants can also constrain the growth of SnO_2 in hydrothermal reactions, leading to very tiny NCs and thus a high surface-to-volume ratio of the hybrid structure ideal for gas sensing. In addition, dopants can generate a large amount of oxygen vacancies and chemisorbed oxygen species, which can further enhance the interaction between NCs and gases. The selectivity of graphene−SnO_2 sensors can be greatly improved by suitable dopants.

Our group recently developed a one-pot strategy to achieve easy and low-cost fabrication of In-doped SnO_2 NCs distributed on the RGO (RGO−IDTO) at a low temperature.[58] To synthesize the hybrids, indium and tin ions were introduced to a GO dispersion in sequence. Then, $NaBH_4$ solution was slowly dropped into the mixture to reduce GO, and RGO−IDTO hybrids were obtained after stirring at 50 °C for 1 h. The morphology characterization of the hybrids indicates that well-defined IDTO NCs with sizes of 2−3 nm were homogenously distributed on the RGO surface. Promising sensing performance was found for highly sensitive and selective detection of NO_2 by using RGO−IDTO hybrids. The addition of indium in SnO_2 significantly enhances the sensitivity to NO_2 compared

dx.doi.org/10.1021/jz400976a | J. Phys. Chem. Lett. 2013, 4, 2441−2454

with that of RGO−SnO_2. The dynamic sensing performance of RGO−IDTO was measured toward various NO_2 concentrations (Figure 8a), and a detection limit of 0.3 ppm was found. The RGO−IDTO sensors also show excellent selectivity toward NO_2 in the presence of other gases, including H_2S, CO, H_2, and NH_3 (Figure 8b), which can be understood as a "superposition effect".

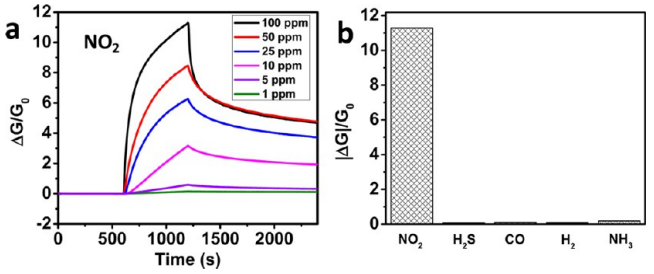

Figure 8. (a) Dynamic sensing response of RGO−IDTO toward different NO_2 concentrations. (b) Comparison of sensitivity to various gases. Reprinted from ref 58 by permission of The Royal Society of Chemistry (RSC).

The properties of graphene−NC hybrids can be engineered by not only functionalizing NCs but also by modifying graphene. Intrinsic graphene has a zero band gap and exhibits a low on−off current ratio when used as the conducting channel in an FET. Fortunately, electronic properties of graphene can be modulated through structural modifications, such as introducing defects into the basal plane and narrowing the graphene sheets to form nanoribbons.[10] Star's group has developed holey RGO (hRGO), which resembles a network of interconnected graphene nanoribbons (GNRs), by enzymatic oxidation of GO followed by chemical reduction.[16] Then, the hRGO flakes were decorated with Pt NCs by pulsed potentiostatic electrodeposition to form a hybrid nanostructure for H_2 detection (Figure 9a). First-principles density functional theory (DFT) calculation was used to investigate the interaction of Pt NCs with the basal plane and the edges of graphene. They found that quinone (C═O)-functionalized C edges of hRGO were highly favorable for metal binding. The gas-sensing performance of the metal NC-decorated hRGO and RGO also was investigated (Figure 9b). Among all of the sensors, only Pt-decorated hRGO (Pt−hRGO) exhibited an improved response toward H_2 gas. The high sensitivity of Pt−hRGO hybrid sensors was attributed to the increased edge-to-plane ratio, the oxygen groups, and the Pt NC decoration. DFT calculations suggested that the spillover of the hydrogen atoms from Pt NCs to the oxygen-functionalized edges of graphene was energetically favorable. The interaction of hydrogen atoms with C═O groups encourages the hydrogen separation on Pt NCs. The Pt−hRGO hybrid sensors have no significant response to CO and CH_4, indicating a high selectivity.

Similarly, "cutting" graphene into nanoribbons can create a sizable band gap due to the lateral confinement of charge carriers.[59] The GNRs also have a large number of edges. All of

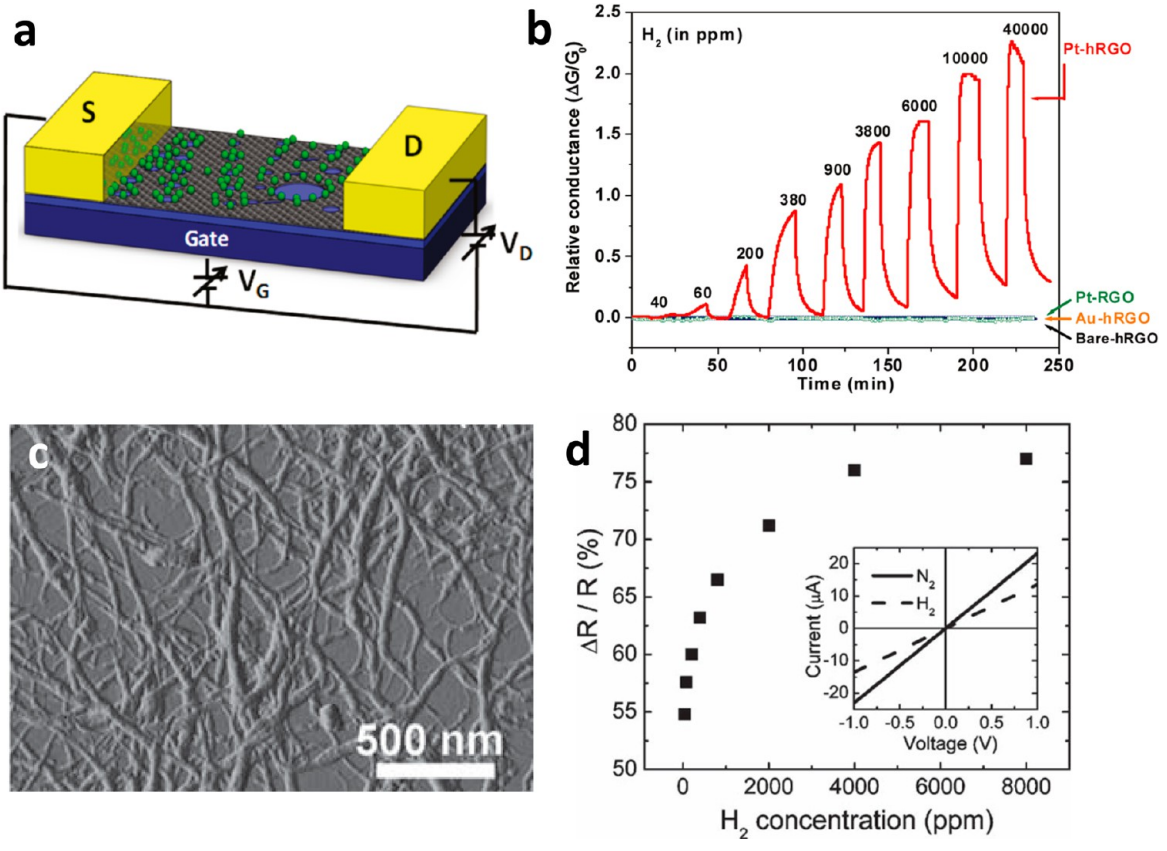

Figure 9. (a) Illustration of a hRGO device decorated with NCs. (b) Relative conductance ($\Delta G/G_0$) versus time curves for H_2 concentrations of 40−40 000 ppm (in N_2) for bare hRGO, Au−hRGO, Pt−hRGO, and Pt−RGO. Reprinted from ref 16. (c) An atomic force microscopy (AFM) image of an MLGN network. (d) The relative resistance response ($\Delta R/R$) as a function of H_2 concentration for the MLGN network sensor. The inset shows the $I-V$ characteristics of the same sensor in N_2 and in 40 ppm H_2. Reprinted with permission from ref 60. Copyright Wiley-VCH, 2010.

dx.doi.org/10.1021/jz400976a | J. Phys. Chem. Lett. 2013, 4, 2441−2454

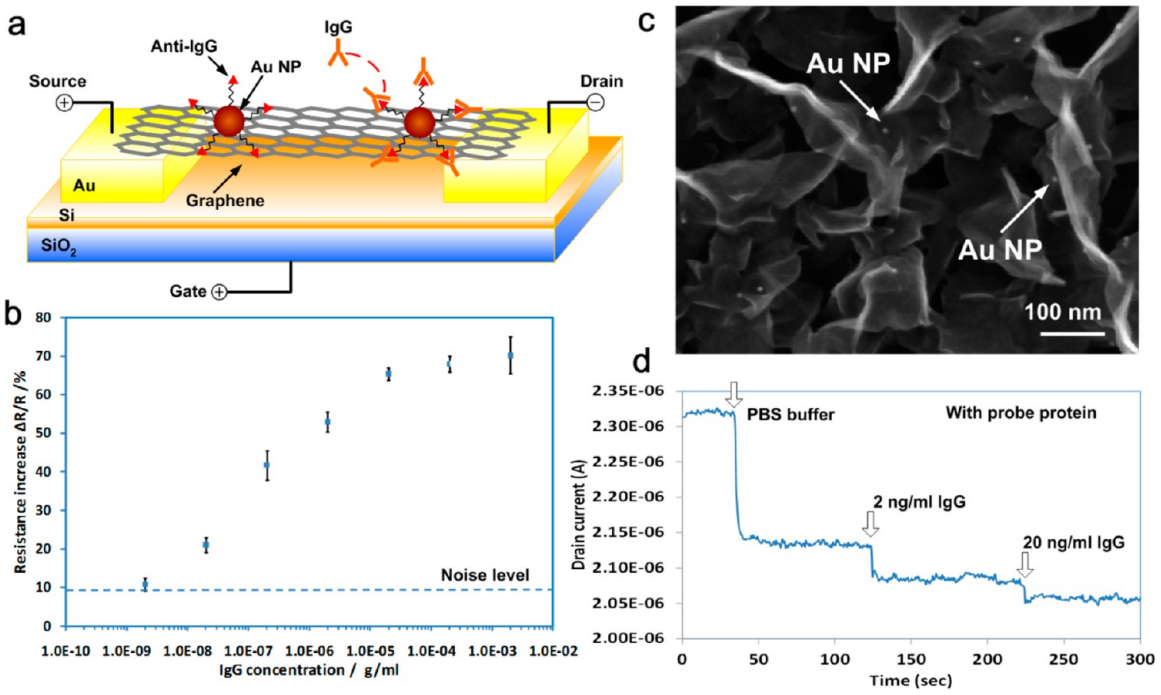

Figure 10. (a) Schematic of a TRGO FET device. (b) Sensor sensitivity versus IgG concentration (g/mL). The dashed line represents the noise level (9.8%) from the buffer solution. Reprinted with permission from ref 17. Copyright Wiley-VCH, 2011. (c) SEM image of the VG network deposited with Au NP-antibody conjugates (top view). (d) Dynamic response of the VG sensor exposed to different concentrations of IgG with probe proteins. Reprinted with permission from ref 62. Copyright Macmillan Publishers Ltd., 2013.

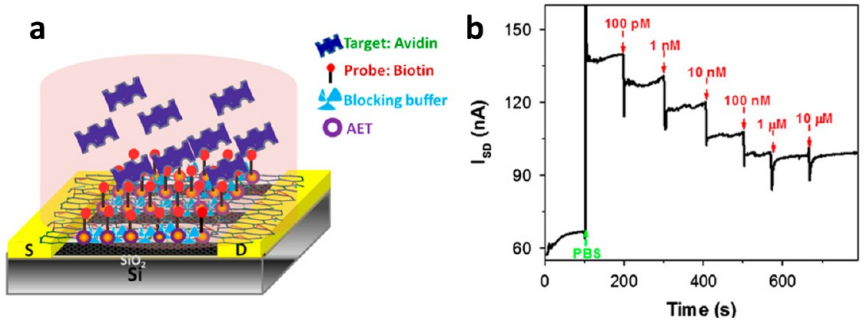

Figure 11. (a) Schematic of a SWCNT/GO/Au NC FET biosensor. (b) Dynamic response of the biosensor for different concentrations of avidin. Reprinted with permission from ref 63. Copyright Elsevier, 2013.

these unique properties greatly benefit the application in gas detection. Johnson et al. have developed a novel H_2 detection device using Pd NC-functionalized multilayer graphene nanoribbon (MLGN) networks.[60] The MLGN networks were fabricated by the dispersion of expanded graphite in a surfactant water solution, following with sonication and filtration. The MLGNs were 3−15 nm thick, 3−13 nm wide, and more than 500 nm long (Figure 9c). A layer of Pd NCs with a size of 1 nm was deposited on MLGNs by e-beam evaporation to obtain the hybrid structure. The Pd-functionalized MLGN networks showed excellent sensitivity to H_2 for concentrations ranging from 40 to 8000 ppm at room temperature (Figure 9d). The hybrid sensors also exhibited fast response/recovery and good repeatability.

Graphene−NC Hybrids for Biosensors. Due to their unique structures and properties, graphene and RGO have been intensely studied as electronic biosensing platforms for biological molecule (e.g., protein and DNA) detection. NCs, especially Au NCs, are widely used in biosensors either as biomolecular linkers or as signal promoters. Au has a high affinity for the chemical groups (e.g., thiol groups) on biological molecules; therefore, it is suitable for linking biomolecules to the graphene. Au NCs could efficiently enhance the electron transfer between target molecules and graphene. In addition, Au NCs also have excellent stability in a buffer or a culture solution.

Our group reported a highly sensitive and selective FET biosensor by using thermally reduced GO (TRGO) decorated with Au NC-antibody conjugates (Figure 10a).[17] The sensing platform provided a reliable and stable structure with TRGO−Au NP-antibodies for target protein detection and effectively prevented the nonspecific protein binding on TRGO with a blocking buffer. The signal was registered by measuring the conductance change of TRGO with the target protein binding. After the introduction of target proteins (IgG), the device had a significant change in conductance. Different concentrations of the target protein were measured (Figure 10b), and a very low detection limit of 2 ng/mL was achieved. A detailed study of

dx.doi.org/10.1021/jz400976a | J. Phys. Chem. Lett. 2013, 4, 2441−2454

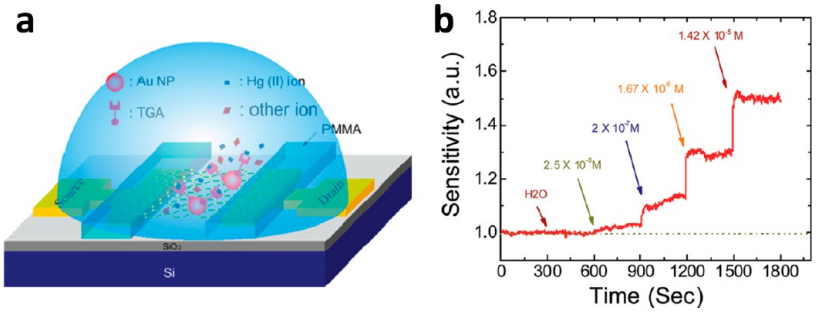

Figure 12. Schematic of the RGO−Au−TGA hybrid water sensor. (b) Dynamic response (sensitivity versus time) of a RGO−Au−TGA hybrid sensor for Hg^{2+} ion concentrations ranging from 2.5×10^{-8} to 1.42×10^{-5} M (V_{ds} = 0.01 V and V_g = 0 V). Reprinted from ref 18.

the system found that the sensor response was significantly dependent on the TRGO base resistance and the areal density of the antibody, suggesting that a single layer graphene fully loaded with probe proteins would be ideal for a protein sensor.[61] When using flat graphene as the conducting channel, the restacking of graphene could lead to a decreased sensing potential. To address this issue, our group developed a hybrid structure of vertically oriented graphene (VG) decorated with Au NC-antibody conjugates for protein detection (Figure 10c and d).[62] The VG sheets were directly grown on gold electrodes using a plasma-enhanced CVD method. The VG−Au NC sensing platform features a fast response and improved stability toward protein detection. This study presents a new method to design and fabricate graphene−NC FET sensors and a promising route for large-scale sensor manufacturing.

Single-walled carbon nanotube (SWCNT) FETs have been successfully used for biomolecule detection because of their excellent sensitivity. However, direct NC decoration on SWCNTs for immobilization of proteins may degrade the gate-dependent performance of the sensor.[63] On the other hand, as GO is insulating and can be extremely thin (~1 nm),[64] it can serve as a passivation layer in the SWCNT FET sensor to prevent the direct attachment of NCs on the CNT and therefore maximize the sensor sensitivity. We recently demonstrated a novel SWCNT FET biosensor (Figure 11a) with a layered structure, SWCNTs as the conducting channel (bottom), GO as an ultrathin dielectric layer covering SWCNTs (middle), and functionalized Au NCs (on top of the GO layer).[63] The Au NCs were functionalized with biotin, serving as the probe for target biomolecules (avidin). The binding event between the target biomolecules and the functionalized Au NCs can cause a top-gating effect on this FET sensor. As a result, the SWCNT/GO/Au NC FET sensor exhibited a sensitive response to the target protein (Figure 11b). In contrast, the sensitivity of SWCNT/Au NC devices (without the GO passivation layer) was considerably lower, confirming the importance of the GO passivation layer for the SWCNT/GO/Au NC FET sensor.

Graphene−NC Hybrids for Water Sensors. Compared with the wide exploration of graphene−NC hybrids in gas sensors and biosensors, there are very few reports on their applications to detect water contaminants (e.g., heavy metal ions and *Escherichia coli* (*E. coli*) bacteria). Our group developed a sensor using RGO decorated with thioglycolic acid (TGA)-functionalized Au NCs for Hg^{2+} detection in water (Figure 12a).[18] The as-prepared RGO−Au−TGA hybrid sensor was highly sensitive to Hg^{2+} and had a detection limit as low as 2.5×10^{-8} M and an instantaneous response on the order of seconds (Figure 12b). TGA ($HS-CH_2-COOH$) consists of a thiol (−C−SH) group and a carboxylic acid (−COOH) group. The thiol group in TGA interacts strongly with gold, which facilitates the anchoring of TGA on Au NPs. On the other hand, the carboxylic acid group acts as a linker to immobilize the Hg^{2+} ion by forming R−COO−(Hg^{2+})−OOC−R chelates.[65] The coupling of Hg^{2+} ions with carboxylic acid groups can change the charge carrier concentration in RGO. To counteract the accumulation of positive charges from Hg^{2+} ions, electrons may transfer from RGO to Au NPs, increasing the concentration of charge carriers (holes) in RGO and thus leading to an increase in conductance. The combination of Au NCs and TGA modification in the hybrids is critical for an excellent sensing performance as our control experiments showed that bare RGO and RGO/Au NC were insensitive to Hg^{2+}. The sensor using RGO and TGA but without a Au NC was also insensitive to Hg^{2+} due to a lack of adhesion between RGO and TGA, verifying the role of Au NCs for anchoring TGA probes in the hybrids. The RGO−Au−TGA sensing platform had relatively weak responses to various other ions (e.g., Na^+, Ca^{2+}, Zn^{2+}, and Fe^{3+}), suggesting its good selectivity for Hg^{2+} detection.

In addition, the TRGO FET sensor was successfully used to detect bacteria for monitoring the water quality. We have developed an *E. coli* sensor with a monolayer of TRGO assembled on aminoethanethiol (AET)-functionalized gold electrodes through electrostatic interactions with ultrasonic assistance.[66] Anti-*E. coli* antibodies were used as receptors through Au NPs on a monolayer of TRGO for the selective detection of *E. coli* cells. The TRGO FET device showed good electronic stability and high sensitivity to *E. coli* cells with a concentration as low as 10 colony-forming units (cfu) per mL. These studies are encouraging and suggest a potential use of graphene−NC FET platforms to detect various contaminants in water.

Future Challenges and Outlook. Significant progress has been made in the research on graphene−NC hybrid structures for energy storage/conversion and sensing applications. Various methods have been used to produce such hybrid structures, and the far-reaching potential of these nanomaterials in energy storage/conversion, sensing, and many other areas has been demonstrated convincingly by numerous reports in the literature. However, challenges remain in further advancing graphene−NC hybrid materials for both fundamental and application-oriented research.

The energy storage/conversion and sensing performance of the graphene−NC structure are determined by electronic, electrochemical, and structural properties of hybrid nanostructures. While understanding of graphene-related materials (e.g., pristine graphene, GO, and RGO) has reached the atomic level, more experimental and theoretical efforts are needed to reveal

dx.doi.org/10.1021/jz400976a | *J. Phys. Chem. Lett.* 2013, 4, 2441−2454

further details of the graphene–NC hybrid systems, particularly the interface between graphene and NCs, upon which the properties of graphene–NC hybrid structures heavily depend. A pressing area for the fundamental aspect of graphene–NC hybrid research is thus to understand the interaction between the two nanocomponents (i.e., graphene and NCs).

A pressing area for the fundamental aspect of graphene–NC hybrid research is thus to understand the interaction between the two nanocomponents (i.e., graphene and NCs).

However, the graphene/NC interface is complex as NCs can interact with graphene through various binding mechanisms (e.g., covalent and noncovalent bonding), and they may attach to graphene at edges and defective sites and/or via functional groups on graphene. The crystallographic orientation of NCs on graphene also influences the graphene/NC interface and the properties of the hybrid structure; however, the control of NC orientation remains a challenging issue for the synthesis of graphene–NC hybrids. In addition, graphene's properties, such as electrochemical reactivity, vary even within a graphene or a chemically modified graphene (GO or RGO) sheet; for example, during the molecular adsorption/desorption process, edges and defects behave very differently compared with the intact region in graphene. As the graphene/NC interface is extremely small, charge transfer across the interface is highly sensitive to the surrounding environment.[50]

The properties of the graphene–NC hybrid highly depend on its structure. For example, the NC size and number density can affect the electronic and electrochemical characteristics of graphene–NC hybrids. The extent to which we can realize the great potential of the graphene–NC hybrid for various applications will heavily rely on our ability to control the graphene–NC structure (e.g., the orientation, morphology, and dispersion of NCs) during the synthesis or postsynthesis process.

The above-mentioned challenges for fundamental research on graphene–NC hybrids open up opportunities for the scientific community. Advanced instrumentation and emerging characterization techniques will help better understand graphene–NC hybrids and provide more insight into their energy storage/conversion and sensing behaviors. For example, multibeam infrared microspectroscopy can be performed at ambient atmospheric pressure[67] and may be used to probe the hybrid structure under realistic working conditions. Materials modeling (e.g., DFT calculations) could also assist in understanding the hybrid structure and provide useful information for future design of hybrids with optimized properties. More experimental and theoretical knowledge about the graphene–NC hybrid structure could lead to synthetic methods for manipulating and engineering the graphene–NC materials with atomic precision, providing a solid foundation for the use of graphene–NC hybrid materials in an even wider spectrum.

For the practical use of graphene–NC hybrid materials in energy and sensing devices, fabrication techniques should be featured with a low cost, a high yield, the capability for scaling up, and high reproducibility. As the safety of nanomaterials is of concern and still under debate, fabricated devices should be robust, suitable for long-term operation, and environmentally friendly. For supercapacitor and LIB electrodes and fuel cell catalysts, the presence of NCs could effectively prevent the restacking and agglomeration of graphene, preserving the accessible surface area of graphene and thus improving the device performance. However, challenges remain about the stability of the hybrid graphene–NC structure, for example, the loss and agglomeration of NCs and the volume change during the charge and discharge process of LIBs. These issues may lead to the detachment of active materials from the current collector and therefore to degradation in the device performance and poor long-term stability. One appealing route to address the stability issue is to create 3D and open graphene structures with NCs wrapped by graphene, which could be realized by growing graphene with templates or by physical deformation of presynthesized graphene. Another issue for LIBs is that electrochemical properties of graphene–NC anodes are currently characterized by fabricating coin cells with a Li foil as the counter electrode. Scaled-up, full-cell tests are needed prior to practical use of graphene–NC anodes in LIBs.

Although a sensor exhibits selectivity to some extent if it gives different signals when exposed to various target analytes one at a time (i.e., differential sensitivity), it is yet to see the "real" selectivity of a graphene–NC sensor when it is exposed to a mixture of target analytes. Fortunately, the graphene–NC hybrid structure is a suitable platform for sensor selectivity modulation. In addition to tuning the selectivity by manipulating the graphene itself, a more adaptable pathway to addressing the selectivity issue is to use NCs that have a specific interaction with target gases/biomolecules to modulate the sensor selectivity (i.e., a large response to a target analyte and a low/no response to interference species). For example, the functionalization of Au NCs with organic or biological ligands has been studied for many years, and a rich library of capture probes is available to selectively target chemicals and biological analytes. Combining graphene with appropriately functionalized NCs could lead to sensors and even sensor arrays capable of selective detection under realistic operating conditions.

Like many other electronic devices based on nanomaterials, another technical challenge for graphene–NC sensors is the performance variation from device to device even though the same fabrication process is followed. Innovative fabrication methods are thus needed to deal with variations among graphene–NC devices due to various fabrication factors. Additionally, new device designs, operating modes, and signal processing procedures could also mitigate the performance variation. Further effort to improve the performance consistency, as well as the sensitivity, stability, and selectivity, of graphene–NC sensors could potentially pave the way for the real-life application of graphene-based sensors.

Given the relatively short history of research in graphene–NC hybrid structures, significant and remarkable developments are expected to take place in the near future. With the improvement in graphene/RGO synthesis methods and the declining cost of graphene materials, graphene–NC hybrid materials are believed to have great potential in energy and sensor applications.

AUTHOR INFORMATION

Corresponding Author

*E-mail: jhchen@uwm.edu.

Author Contributions

[§]S.C., S.M., and G.L. contributed equally.

Author Contributions

The manuscript was written through contributions of all authors. All authors have given approval to the final version of the manuscript.

Notes

The authors declare no competing financial interest.

Biographies

Shumao Cui received his Ph.D. in Mechanical Engineering from the University of Wisconsin—Milwaukee (UWM) in 2013 and is currently a postdoctoral fellow at UWM. His research interests include the synthesis of NCs, synthesis of nanohybrids combining nanocarbons (graphene and CNTs) with NCs, and developing environment and energy applications using nanomaterials.

Shun Mao received his doctoral degree in Mechanical Engineering from UWM in 2010 for the study of hybrid nanomaterials for biosensing applications. After graduation, he worked as a project director at NanoAffix Science, LLC for a hydrogen sensor project from 2011 to 2012. He is currently a postdoctoral fellow at UWM. His research is focused on nanomaterials/nanostructures for energy, biomedical, and environmental applications.

Ganhua Lu is an Assistant Professor of Mechanical Engineering at the University of Alaska Anchorage. His research is focused on synthesis of hybrid nanostructures consisting of nanocarbons (i.e., graphene and CNTs) decorated with functional nanocrystals and their use for environmental and energy devices.

Junhong Chen is a Professor of Mechanical Engineering and Professor of Materials Science and Engineering at UWM. His research interests lie in NC synthesis and assembly; nanocarbons (i.e., graphene and CNTs) and hybrid nanomaterials; nanostructure-based gas sensors, water sensors, and biosensors; and nanocarbon-based hybrid nanomaterials for sustainable energy and environment (http://www.uwm.edu/nsee/).

■ ACKNOWLEDGMENTS

J.C. gratefully acknowledges financial support from the National Science Foundation (IIP-1128158 and CMMI-0900509) and the U.S. Department of Energy (DE-EE-0003208). G.L. thanks UAA for a Faculty Development Grant.

■ ABBREVIATIONS

NC, nanocrystal; 2D, two-dimensional; 3D, three-dimensional; RGO, reduced graphene oxide; NG, nitrogen-doped graphene; SERS, surface-enhanced Raman scattering; FET, field-effect transistor; hRGO, holey RGO; DFT, density functional theory; GNRs, graphene nanoribbons; MLGN, multilayer graphene nanoribbon; AFM, atomic force microscopy; SEM, scanning electron microscopy; TEM, transmission electron microscopy; TRGO, thermally reduced graphene oxide; VG, vertically oriented graphene; CVD, chemical vapor deposition; SWCNT, single-walled carbon nanotube; MWCNT, multiwalled carbon nanotube; AET, aminoethanethiol; *E. coli*, *Escherichia coli*; cfu, colony-forming units; EC, electrochemical capacitor; EDLC, electric double-layer capacitor; CG, crumpled graphene; LIBs, lithium ion batteries; EVs, electric vehicles; ORR, oxygen reduction reaction; rmGO, reduced mildly oxidized graphene oxide; CV, cyclic voltammetry; DSSC, dye-sensitized solar cell; QDSSC, quantum-dot-sensitized solar cell

■ REFERENCES

(1) Novoselov, K. S.; Geim, A. K.; Morozov, S. V.; Jiang, D.; Zhang, Y.; Dubonos, S. V.; Grigorieva, I. V.; Firsov, A. A. Electric Field Effect in Atomically Thin Carbon Films. *Science* **2004**, *306*, 666−669.
(2) Zhang, Y. B.; Tan, Y. W.; Stormer, H. L.; Kim, P. Experimental Observation of the Quantum Hall Effect and Berry's Phase in Graphene. *Nature* **2005**, *438*, 201−204.
(3) Balandin, A. A.; Ghosh, S.; Bao, W. Z.; Calizo, I.; Teweldebrhan, D.; Miao, F.; Lau, C. N. Superior Thermal Conductivity of Single-Layer Graphene. *Nano Lett.* **2008**, *8*, 902−907.
(4) Frank, I. W.; Tanenbaum, D. M.; Van der Zande, A. M.; McEuen, P. L. Mechanical Properties of Suspended Graphene Sheets. *J. Vac. Sci. Technol., B* **2007**, *25*, 2558−2561.
(5) Novoselov, K. S.; Fal'ko, V. I.; Colombo, L.; Gellert, P. R.; Schwab, M. G.; Kim, K. A Roadmap for Graphene. *Nature* **2012**, *490*, 192−200.
(6) Lu, G.; Mao, S.; Park, S.; Ruoff, R. S.; Chen, J. Facile, Noncovalent Decoration of Graphene Oxide Sheets with Nanocrystals. *Nano Res.* **2009**, *2*, 192−200.
(7) Alivisatos, A. P. Perspectives on the Physical Chemistry of Semiconductor Nanocrystals. *J. Phys. Chem.* **1996**, *100*, 13226−13239.
(8) Kamat, P. V. Quantum Dot Solar Cells. Semiconductor Nanocrystals as Light Harvesters. *J. Phys. Chem. C* **2008**, *112*, 18737−18753.
(9) Dreyer, D. R.; Ruoff, R. S.; Bielawski, C. W. From Conception to Realization: An Historial Account of Graphene and Some Perspectives for Its Future. *Angew. Chem., Int. Ed.* **2010**, *49*, 9336−9344.
(10) Lu, G. H.; Yu, K. H.; Wen, Z. H.; Chen, J. H. Semiconducting Graphene: Converting Graphene from Semimetal to Semiconductor. *Nanoscale* **2013**, *5*, 1353−1368.
(11) Geim, A. K.; Novoselov, K. S. The Rise of Graphene. *Nat. Mater.* **2007**, *6*, 183−191.
(12) Liang, Y.; Li, Y.; Wang, H.; Zhou, J.; Wang, J.; Regier, T.; Dai, H. Co_3O_4 Nanocrystals on Graphene as a Synergistic Catalyst for Oxygen Reduction Reaction. *Nat. Mater.* **2011**, *10*, 780−786.
(13) Mao, S.; Wen, Z. H.; Kim, H.; Lu, G. H.; Hurley, P.; Chen, J. H. A General Approach to One-Pot Fabrication of Crumpled Graphene-Based Nanohybrids for Energy Applications. *ACS Nano* **2012**, *6*, 7505−7513.
(14) Wen, Z. H.; Cui, S. M.; Kim, H.; Mao, S.; Yu, K. H.; Lu, G. H.; Pu, H. H.; Mao, O.; Chen, J. H. Binding Sn-Based Nanoparticles on Graphene as the Anode of Rechargeable Lithium-Ion Batteries. *J. Mater. Chem.* **2012**, *22*, 3300−3306.
(15) Mao, S.; Cui, S. M.; Lu, G. H.; Yu, K. H.; Wen, Z. H.; Chen, J. H. Tuning Gas-Sensing Properties of Reduced Graphene Oxide Using Tin Oxide Nanocrystals. *J. Mater. Chem.* **2012**, *22*, 11009−11013.
(16) Vedala, H.; Sorescu, D. C.; Kotchey, G. P.; Star, A. Chemical Sensitivity of Graphene Edges Decorated with Metal Nanoparticles. *Nano Lett.* **2011**, *11*, 2342−2347.
(17) Mao, S.; Lu, G. H.; Yu, K. H.; Bo, Z.; Chen, J. H. Specific Protein Detection Using Thermally Reduced Graphene Oxide Sheet Decorated with Gold Nanoparticle-Antibody Conjugates. *Adv. Mater.* **2010**, *22*, 3521−3526.
(18) Chen, K. H.; Lu, G. H.; Chang, J. B.; Mao, S.; Yu, K. H.; Cui, S. M.; Chen, J. H. Hg(II) Ion Detection Using Thermally Reduced Graphene Oxide Decorated with Functionalized Gold Nanoparticles. *Anal. Chem.* **2012**, *84*, 4057−4062.
(19) Lightcap, I. V.; Kamat, P. V. Graphitic Design: Prospects of Graphene-Based Nanocomposites for Solar Energy Conversion, Storage, and Sensing. *Acc. Chem. Res.* **2012**, DOI: 10.1021/ar300248f.
(20) Huang, X.; Qi, X.; Boey, F.; Zhang, H. Graphene-Based Composites. *Chem. Soc. Rev.* **2012**, *41*, 666−686.
(21) Simon, P.; Gogotsi, Y. Materials for Electrochemical Capacitors. *Nat. Mater.* **2008**, *7*, 845−854.
(22) Stoller, M. D.; Park, S. J.; Zhu, Y. W.; An, J. H.; Ruoff, R. S. Graphene-Based Ultracapacitors. *Nano Lett.* **2008**, *8*, 3498−3502.
(23) Zhao, Y.; Hu, C.; Hu, Y.; Cheng, H.; Shi, G.; Qu, L. A Versatile, Ultralight, Nitrogen-Doped Graphene Framework. *Angew. Chem., Int. Ed.* **2012**, *51*, 11371−11375.

(24) Xia, J. L.; Chen, F.; Li, J. H.; Tao, N. J. Measurement of the Quantum Capacitance of Graphene. *Nat. Nanotechnol.* **2009**, *4*, 505−509.
(25) Bai, S.; Shen, X. Graphene−Inorganic Nanocomposites. *RSC Adv.* **2012**, *2*, 64−98.
(26) Toupin, M.; Brousse, T.; Bélanger, D. Charge Storage Mechanism of MnO_2 Electrode Used in Aqueous Electrochemical Capacitor. *Chem. Mater.* **2004**, *16*, 3184−3190.
(27) Yu, G.; Hu, L.; Vosgueritchian, M.; Wang, H.; Xie, X.; McDonough, J. R.; Cui, X.; Cui, Y.; Bao, Z. Solution-Processed Graphene/MnO_2 Nanostructured Textiles for High-Performance Electrochemical Capacitors. *Nano Lett.* **2011**, *11*, 2905−2911.
(28) He, Y.; Chen, W.; Li, X.; Zhang, Z.; Fu, J.; Zhao, C.; Xie, E. Freestanding Three-Dimensional Graphene/MnO_2 Composite Networks as Ultralight and Flexible Supercapacitor Electrodes. *ACS Nano* **2013**, *7*, 174−182.
(29) Etacheri, V.; Marom, R.; Elazari, R.; Salitra, G.; Aurbach, D. Challenges in the Development of Advanced Li-Ion Batteries: A Review. *Energy Environ. Sci.* **2011**, *4*, 3243−3262.
(30) Dahn, J. R.; Zheng, T.; Liu, Y.; Xue, J. S. Mechanisms for Lithium Insertion in Carbonaceous Materials. *Science* **1995**, *270*, 590−593.
(31) Chiang, Y.-M. Building A Better Battery. *Science* **2010**, *330*, 1485−1486.
(32) Courtney, I. A.; Dahn, J. R. Electrochemical and In Situ X-ray Diffraction Studies of the Reaction of Lithium with Tin Oxide Composites. *J. Electrochem. Soc.* **1997**, *144*, 2045−2052.
(33) Yang, S.; Sun, Y.; Chen, L.; Hernandez, Y.; Feng, X.; Muellen, K. Porous Iron Oxide Ribbons Grown on Graphene for High-Performance Lithium Storage. *Sci. Rep.* **2012**, *2*, Article 427.
(34) Zhao, X.; Hayner, C. M.; Kung, M. C.; Kung, H. H. In-Plane Vacancy-Enabled High-Power Si−Graphene Composite Electrode for Lithium-Ion Batteries. *Adv. Energy Mater.* **2011**, *1*, 1079−1084.
(35) Chan, C. K.; Peng, H.; Liu, G.; McIlwrath, K.; Zhang, X. F.; Huggins, R. A.; Cui, Y. High-Performance Lithium Battery Anodes Using Silicon Nanowires. *Nat. Nanotechnol.* **2008**, *3*, 31−35.
(36) Choi, B. G.; Chang, S.-J.; Lee, Y. B.; Bae, J. S.; Kim, H. J.; Huh, Y. S. 3D Heterostructured Architectures of Co_3O_4 Nanoparticles Deposited on Porous Graphene Surfaces for High Performance of Lithium Ion Batteries. *Nanoscale* **2012**, *4*, 5924−5930.
(37) Lee, J. K.; Smith, K. B.; Hayner, C. M.; Kung, H. H. Silicon Nanoparticles−Graphene Paper Composites for Li Ion Battery Anodes. *Chem. Commun.* **2010**, *46*, 2025−2027.
(38) Zhu, X.; Zhu, Y.; Murali, S.; Stoller, M. D.; Ruoff, R. S. Nanostructured Reduced Graphene Oxide/Fe_2O_3 Composite as a High-Performance Anode Material for Lithium Ion Batteries. *ACS Nano* **2011**, *5*, 3333−3338.
(39) Wu, Z.-S.; Ren, W.; Wen, L.; Gao, L.; Zhao, J.; Chen, Z.; Zhou, G.; Li, F.; Cheng, H.-M. Graphene Anchored with Co_3O_4 Nanoparticles as Anode of Lithium Ion Batteries with Enhanced Reversible Capacity and Cyclic Performance. *ACS Nano* **2010**, *4*, 3187−3194.
(40) Gasteiger, H. A.; Markovic, N. M. Just a Dream or Future Reality? *Science* **2009**, *324*, 48−49.
(41) Stamenkovic, V. R.; Mun, B. S.; Arenz, M.; Mayrhofer, K. J. J.; Lucas, C. A.; Wang, G.; Ross, P. N.; Markovic, N. M. Trends in Electrocatalysis on Extended and Nanoscale Pt−Bimetallic Alloy Surfaces. *Nat. Mater.* **2007**, *6*, 241−247.
(42) Bashyam, R.; Zelenay, P. A Class of Non-precious Metal Composite Catalysts for Fuel Cells. *Nature* **2006**, *443*, 63−66.
(43) Winther-Jensen, B.; Winther-Jensen, O.; Forsyth, M.; MacFarlane, D. R. High Rates of Oxygen Reduction over a Vapor Phase−Polymerized PEDOT Electrode. *Science* **2008**, *321*, 671−674.
(44) Gong, K.; Du, F.; Xia, Z.; Durstock, M.; Dai, L. Nitrogen-Doped Carbon Nanotube Arrays with High Electrocatalytic Activity for Oxygen Reduction. *Science* **2009**, *323*, 760−764.
(45) Qu, L.; Liu, Y.; Baek, J.-B.; Dai, L. Nitrogen-Doped Graphene as Efficient Metal-Free Electrocatalyst for Oxygen Reduction in Fuel Cells. *ACS Nano* **2010**, *4*, 1321−1326.
(46) Li, Y.; Zhou, W.; Wang, H.; Xie, L.; Liang, Y.; Wei, F.; Idrobo, J.-C.; Pennycook, S. J.; Dai, H. An Oxygen Reduction Electrocatalyst Based on Carbon Nanotube−Graphene Complexes. *Nat. Nanotechnol.* **2012**, *7*, 394−400.
(47) Yang, S.; Feng, X.; Wang, X.; Muellen, K. Graphene-Based Carbon Nitride Nanosheets as Efficient Metal-Free Electrocatalysts for Oxygen Reduction Reactions. *Angew. Chem., Int. Ed.* **2011**, *50*, 5339−5343.
(48) Sun, S.; Gao, L.; Liu, Y. Enhanced Dye-Sensitized Solar Cell Using Graphene−TiO_2 Photoanode Prepared by Heterogeneous Coagulation. *Appl. Phys. Lett.* **2010**, *96*, 083113.
(49) Lightcap, I. V.; Kamat, P. V. Fortification of CdSe Quantum Dots with Graphene Oxide. Excited State Interactions and Light Energy Conversion. *J. Am. Chem. Soc.* **2012**, *134*, 7109−7116.
(50) Yu, K. H.; Lu, G. H.; Mao, S.; Chen, K.; Kim, H.; Wen, Z. H.; Chen, J. H. Selective Deposition of CdSe Nanoparticles on Reduced Graphene Oxide to Understand Photoinduced Charge Transfer in Hybrid Nanostructures. *ACS Appl. Mater. Interfaces* **2011**, *3*, 2703−2709.
(51) Wen, Z. H.; Cui, S. M.; Pu, H. H.; Mao, S.; Yu, K. H.; Feng, X. L.; Chen, J. H. Metal Nitride/Graphene Nanohybrids: General Synthesis and Multifunctional Titanium Nitride/Graphene Electrocatalyst. *Adv. Mater.* **2011**, *23*, 5445−5450.
(52) Schedin, F.; Geim, A. K.; Morozov, S. V.; Hill, E. W.; Blake, P.; Katsnelson, M. I.; Novoselov, K. S. Detection of Individual Gas Molecules Adsorbed on Graphene. *Nat. Mater.* **2007**, *6*, 652−655.
(53) Yu, K.; Lu, G.; Bo, Z.; Mao, S.; Chen, J. Carbon Nanotube with Chemically Bonded Graphene Leaves for Electronic and Optoelectronic Applications. *J. Phys. Chem. Lett.* **2011**, *2*, 1556−1562.
(54) Yu, K.; Wang, P.; Lu, G.; Chen, K.-H.; Bo, Z.; Chen, J. Patterning Vertically Oriented Graphene Sheets for Nanodevice Applications. *J. Phys. Chem. Lett.* **2011**, *2*, 537−542.
(55) Cui, S. M.; Pu, H. H.; Lu, G. H.; Wen, Z. H.; Mattson, E. C.; Hirschmugl, C.; Gajdardziska-Josifovska, M.; Weinert, M.; Chen, J. H. Fast and Selective Room-Temperature Ammonia Sensors Using Silver Nanocrystal-Functionalized Carbon Nanotubes. *ACS Appl. Mater. Interfaces* **2012**, *4*, 4898−4904.
(56) Cui, S. M.; Mao, S.; Wen, Z. H.; Chang, J. B.; Zhang, Y.; Chen, J. H. Controllable Synthesis of Silver Nanoparticle-Decorated Reduced Graphene Oxide Hybrids for Ammonia Detection. *Analyst* **2013**, *138*, 2877−2882.
(57) Russo, P. A.; Donato, N.; Leonardi, S. G.; Baek, S.; Conte, D. E.; Neri, G.; Pinna, N. Room-Temperature Hydrogen Sensing with Heteronanostructures Based on Reduced Graphene Oxide and Tin Oxide. *Angew. Chem., Int. Ed.* **2012**, *51*, 11053−11057.
(58) Cui, S. M.; Wen, Z. H.; Mattson, E. C.; Mao, S.; Chang, J. B.; Weinert, M.; Hirschmugl, C. J.; Gajdardziska-Josifovska, M.; Chen, J. H. Indium-Doped SnO_2 Nanoparticle−Graphene Nanohybrids: Simple One-Pot Synthesis and Their Selective Detection of NO_2. *J. Mater. Chem. A* **2013**, *1*, 4462−4467.
(59) Han, M. Y.; Ozyilmaz, B.; Zhang, Y. B.; Kim, P. Energy Band-Gap Engineering of Graphene Nanoribbons. *Phys. Rev. Lett.* **2007**, *98*, 206805.
(60) Johnson, J. L.; Behnam, A.; Pearton, S. J.; Ural, A. Hydrogen Sensing Using Pd-Functionalized Multi-Layer Graphene Nanoribbon Networks. *Adv. Mater.* **2010**, *22*, 4877−4880.
(61) Mao, S.; Yu, K. H.; Lu, G. H.; Chen, J. H. Highly Sensitive Protein Sensor Based on Thermally-Reduced Graphene Oxide Field-Effect Transistor. *Nano Res.* **2011**, *4*, 921−930.
(62) Mao, S.; Yu, K. H.; Chang, J. B.; Steeber, D. A.; Ocola, L. E.; Chen, J. H. Direct Growth of Vertically-Oriented Graphene for Field-Effect Transistor Biosensor. *Sci. Rep.* **2013**, *3*, 1696.
(63) Chang, J. B.; Mao, S.; Zhang, Y.; Cui, S. M.; Steeber, D. A.; Chen, J. H. Single-Walled Carbon Nanotube Field-Effect Transistors with Graphene Oxide Passivation for Fast, Sensitive, and Selective Protein detection. *Biosens. Bioelectron.* **2013**, *42*, 186−192.
(64) Mao, S.; Pu, H. H.; Chen, J. H. Graphene Oxide and Its Reduction: Modeling and Experimental Progress. *RSC Adv.* **2012**, *2*, 2643−2662.

(65) Chen, J. L.; Zheng, A. F.; Chen, A. H.; Gao, Y. C.; He, C. Y.; Kai, X. M.; Wu, G. H.; Chen, Y. C. A Functionalized Gold Nanoparticles and Rhodamine 6G Based Fluorescent Sensor for High Sensitive and Selective Detection of Mercury(II) in Environmental Water Samples. *Anal. Chim. Acta* **2007**, *599*, 134−142.
(66) Chang, J. B.; Mao, S.; Zhang, Y.; Cui, S. M.; Zhou, G. H.; Wu, X. G.; Yang, C. H.; Chen, J. H. Ultrasonic-Assisted Self-Assembly of Monolayer Graphene Oxide for Rapid Detection of Escherichia Coli Bacteria. *Nanoscale* **2013**, *5*, 3620−3626.
(67) Nasse, M. J.; Walsh, M. J.; Mattson, E. C.; Reininger, R.; Kajdacsy-Balla, A.; Macias, V.; Bhargava, R.; Hirschmugl, C. J. High-Resolution Fourier-Transform Infrared Chemical Imaging with Multiple Synchrotron Beams. *Nat. Methods* **2011**, *8*, 413−U58.